USGS-OFR-82-973

UNITED STATES
DEPARTMENT OF THE INTERIOR
GEOLOGICAL SURVEY

PRELIMINARY INTERPRETATION OF THERMAL DATA FROM THE NEVADA TEST SITE

Open-File Report 82-973

1982

Prepared by the U.S. Geological Survey

for the

Nevada Operations Office
U.S. Department of Energy
(Interagency Agreement DE-AI08-78ET44802)

USGS-OFR-82-973

UNITED STATES
DEPARTMENT OF THE INTERIOR
GEOLOGICAL SURVEY

PRELIMINARY INTERPRETATION OF THERMAL DATA FROM THE NEVADA TEST SITE

by

J. H. Sass and Arthur H. Lachenbruch

Open-File Report 82-973

1982

Abstract

Analysis of data from 60 wells in and around the Nevada Test Site, including 16 in the Yucca Mountain area, indicates a thermal regime characterized by large vertical and lateral gradients in heat flow. Estimates of heat flow indicate considerable variation on both regional and local scales. The variations are attributable primarily to hydrologic processes involving interbasin flow with a vertical component of (seepage) velocity (volume flux) of a few mm/yr. Apart from indicating a general downward movement of water at a few mm/yr, the results from Yucca Mountain are as yet inconclusive.

INTRODUCTION

The Geothermal Studies Project, USGS, has been periodically measuring temperatures in holes drilled in and near the Nevada Test Site (NTS) in southern Nevada (fig. 1). Our primary motivation has been the measurement of the earth's heat flow. Thus, when we examined temperature profiles within the context of heat flow in the western United States (Sass and others, 1971), we discarded most of the data we had obtained as unsuitable owing to hydrologic disturbances to the conductive heat-flow field. Recently (Lachenbruch and Sass, 1977), we have attempted to refine our interpretation of the variation of heat flow in the western U.S. In particular, we have sought to explain much of the scatter in heat flow within the Great Basin in terms of local water circulation. In addition, we have interpreted the large area of anomalously low heat flow (Eureka Low, EL, fig. 1) as reflecting regional water flow with a downward (seepage) velocity component on the order of a few mm/y (Lachenbruch and Sass, 1977) consistent with regional hydrologic studies (see Winograd and Thordarson, 1975). The regional heat flow from beneath the zone of hydrologic disturbance in the Eureka Low may be the same as that characteristic of the Great Basin in general ($\sim$80 mWm^{-2}, or $\sim$2 HFU) or it could be as high as $\sim$100 mWm^{-2} ($\sim$2.5 HFU).

In view of the importance of hydrologic processes in determining the suitability of proposed repository sites, and because thermal measurements are extremely sensitive to these processes, we have re-examined our existing data and obtained additional data from Syncline Ridge near the Eleana Range, hole U15K in the Climax Stock, and from all available wells near Yucca Mountain (fig. 2). In this section, we briefly review the thermal data from approximately 60 wells and their implications for regional heat flow. We also

examine in more detail the thermal data from the Yucca Mountain site and their implications for vertical water flow within and adjacent to the proposed nuclear waste repository.

Acknowledgments. Temperature measurements were made by Gordon Greene, Fred Grubb, Tom Moses, Bob Munroe, and Gene Smith. Conductivities were measured by Bob Munroe and Gene Smith. We are grateful to W. E. Wilson and Rick Waddell for their helpful comments and suggestions.

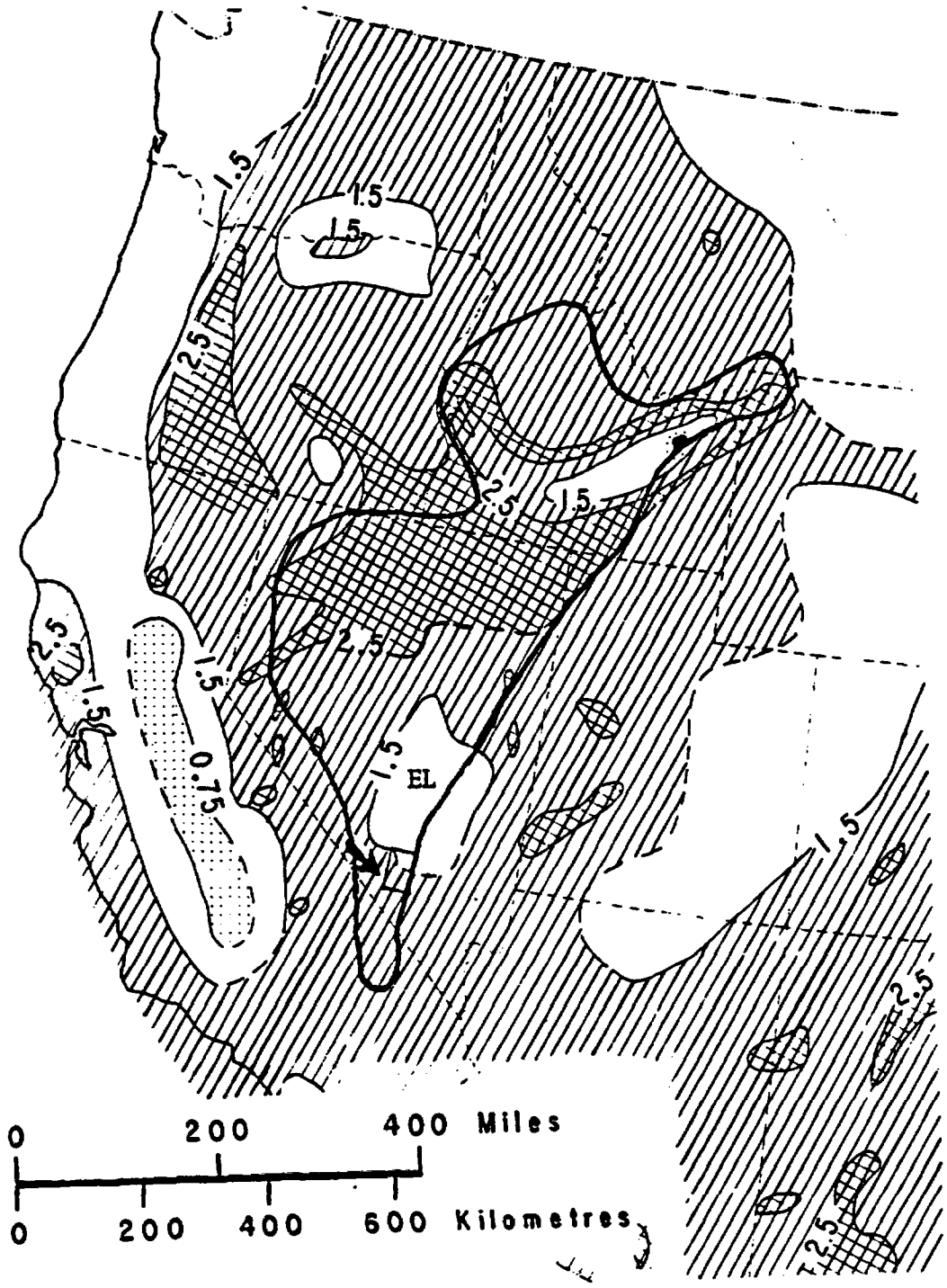

Figure 1. Map of western United States showing heat-flow contours (in HFU) 1 heat-flow unit (HFU) = 41.86 mWm^{-2}. EL is Eureka Low. Arrow indicates outline of approximate boundaries of the Nevada Test Site (NTS). Heavy line is 2.5 HFU contour, based on the empirical relation between silica temperatures and heat flow (Swanberg and Morgan, 1978).

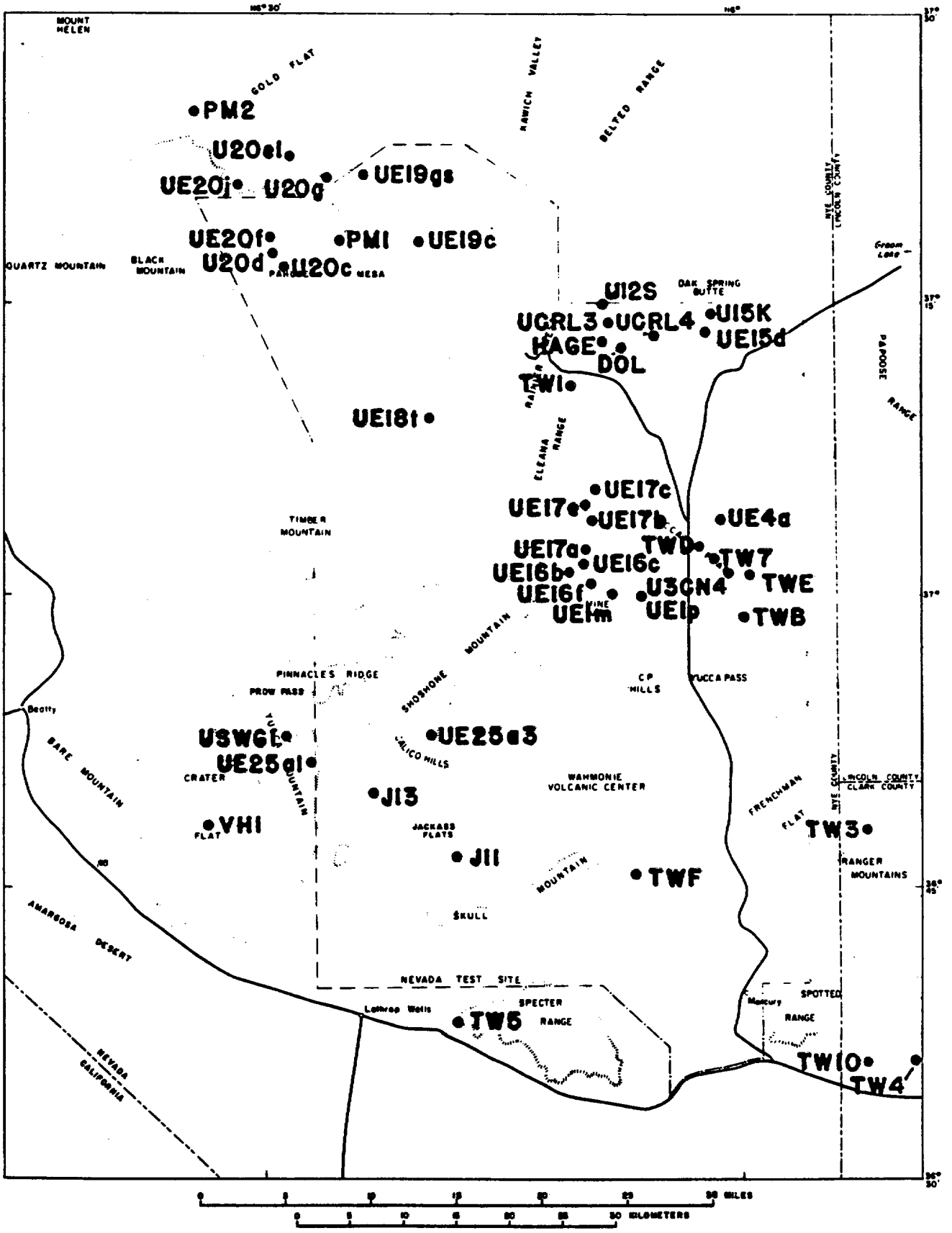

Figure 2. Map of the test-site region showing locations of wells discussed in the text.

REGIONAL HEAT FLOW

Available heat-flow data from the NTS region are summarized in table 1 and figure 3. The data described as "USGS Unpublished" are preliminary and are subject to minor revision (± a few percent) upon further study. The data (fig. 3) indicate a typical Basin-and-Range distribution of heat flow in the region immediately surrounding Mercury but a rather complex situation to the north and west. The complexity of the thermal regime is further demonstrated, and can be explained to some extent, by consideration of all temperature data within the region (fig. 2). These data are presented as a series of composite temperature-depth plots ("worm diagrams") for different areas within the region in figures 4 through 8 and 10.

Beneath Pahute Mesa (fig. 4), temperature gradients are fairly low (~20 to 25°C/km), and the tuffs within which the wells were drilled have low thermal conductivities (1 to 1.5 $Wm^{-1} K^{-1}$) resulting in anomalously low values of regional heat flow. The deepest log we obtained from NTS was that in Ue20f (fig. 4). In the upper 1.5 km, the temperature gradient is 26°C/km and the calculated conductive heat flow is less than 40 mWm^{-2}. Below 1.5 km, there is a zone extending to nearly 3 km that is probably disturbed by a complex combination of lateral and vertical water flow. Below 3 km, the temperature profile is linear, and the gradient is 37°C/km. Thermal conductivities in this section are not well characterized, but reasonable values would result in heat-flow values between 80 and 100 mWm^{-2} which is typical of the Basin and Range Province in general. The implication here is that water is carrying off much of the earth's heat in the upper 3 km and delivering it elsewhere. Well PM-2 is a possible exception. Its temperature profile (fig. 4) might indicate regional heat flow or possibly just a local upwelling of convecting water.

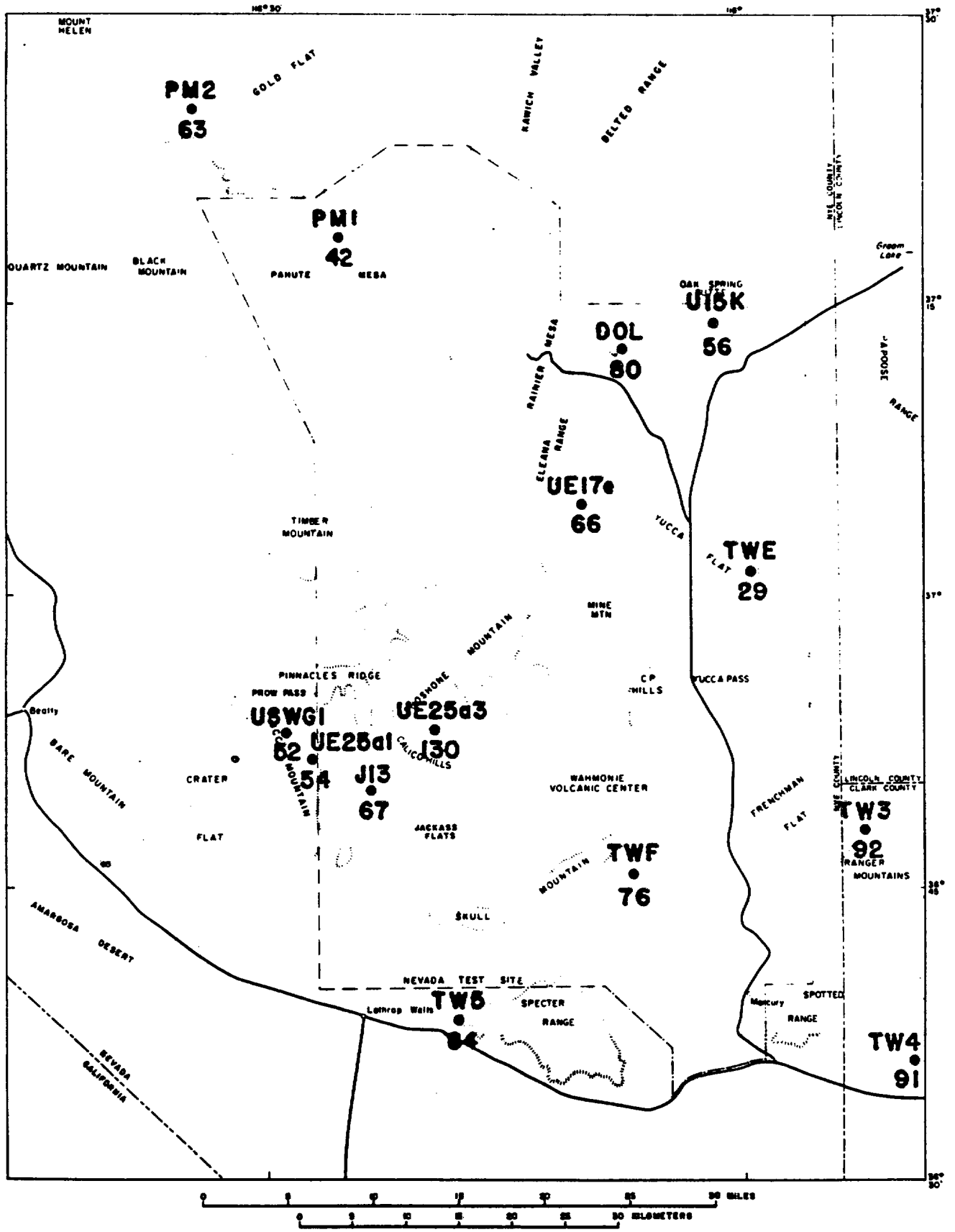

Figure 3. Regional heat-flow values within and adjacent to the Nevada Test Site.

TABLE 1. Heat-flow determinations in and adjacent to the Nevada Test Site (see Figures 2 and 3 for locations)

Well	Heat flow		Reference
	mWm^{-2}	HFU	
PM2	63	1.5	Sass and others, 1971
PM1	42	1.0	Sass and others, 1971
DOL	80	1.9	Sass and others, 1971
U15K	56	1.3	USGS unpublished
Ue17e	66	1.58	USGS unpublished
TWE	29	0.7	Sass and others, 1971
J-13	67	1.6	Sass and others, 1971
Ue25a1	54	1.3	Sass and others, 1980
Ue25b1	47	1.1	USGS unpublished
Ue25a3	130	3.1	Sass and others, 1980
USWG1*	52	1.25	Table 2, this paper
TWF	76	1.81	Sass and others, 1971
TW3	92	2.2	Sass and others, 1971
TW5	84	2.0	Sass and others, 1971
TW4	91	2.2	Sass and others, 1971

*Average heat flow in lowermost ~600 m.

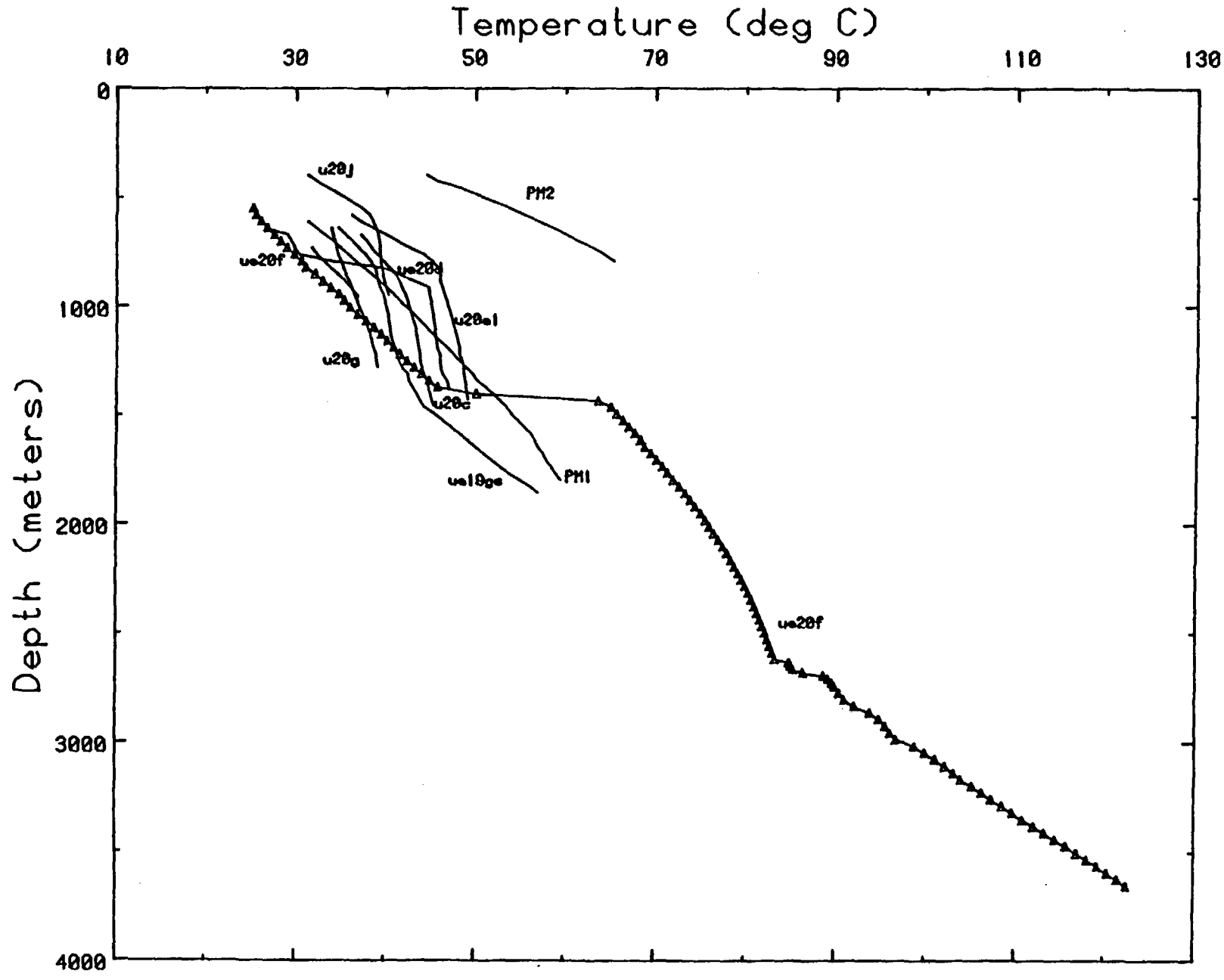

Figure 4. Composite Temperature Profile, Pahute Mesa

Consideration of temperatures from other areas of the NTS (figs. 5 through 8) also suggests lateral variations in heat flow that can be attributed largely to lateral and vertical water movement with vertical seepage velocities probably on the order of 1-10 mm/y.

The most reliable "flux plates" for determination of regional heat flow generally have been granitic bodies. Unfortunately, we have only one such determination (U15k, fig. 3), and even it is uncertain because the hole is relatively shallow (~260 m), and we have only one determination of thermal conductivity. The best documented heat-flux value in this region is that for UE17e (figs. 3 and 7) which was drilled in argillites of the Eleana Formation. This is the only well in this entire study for which we can rule out vertical water movement in the hole, as the access casing was completely grouted in. In other wells, some or all of the perturbations to the steady-state conductive thermal regime may be the result of water movement in the annulus between casing and borehole wall rather than water movement in the formation. Fortunately, however, it is usually possible to distinguish between the two types of flow on the basis of the shape of the disturbed temperature profile.

To characterize adequately the heat flow in this region, we require several holes to depths of several hundred meters, preferably drilled in granitic rocks, and with the annulus between access casing and borehole wall completely sealed off by grout or a similar medium.

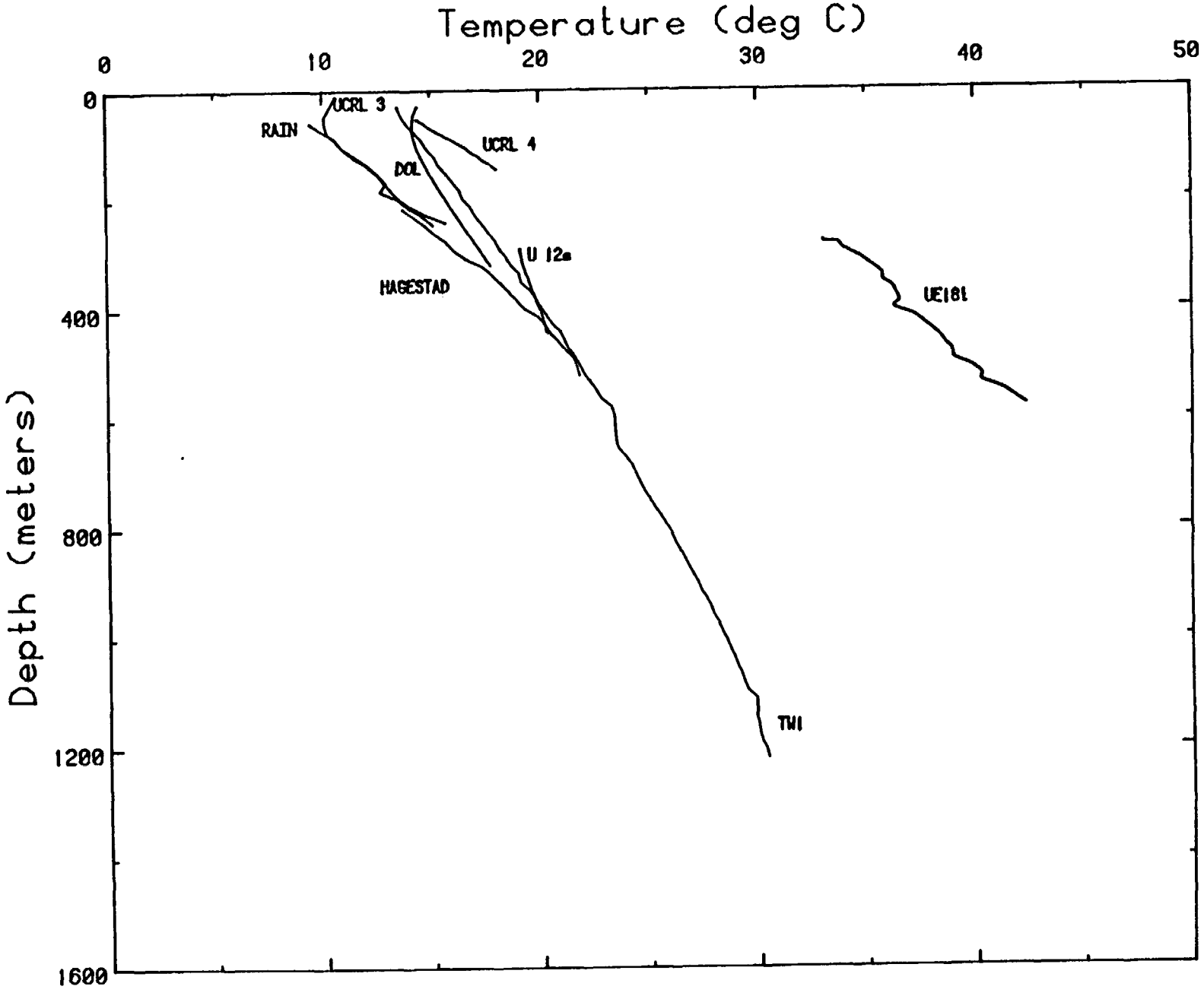

Figure 5. Composite Temperature Profile for Rainier Mesa & Environs.

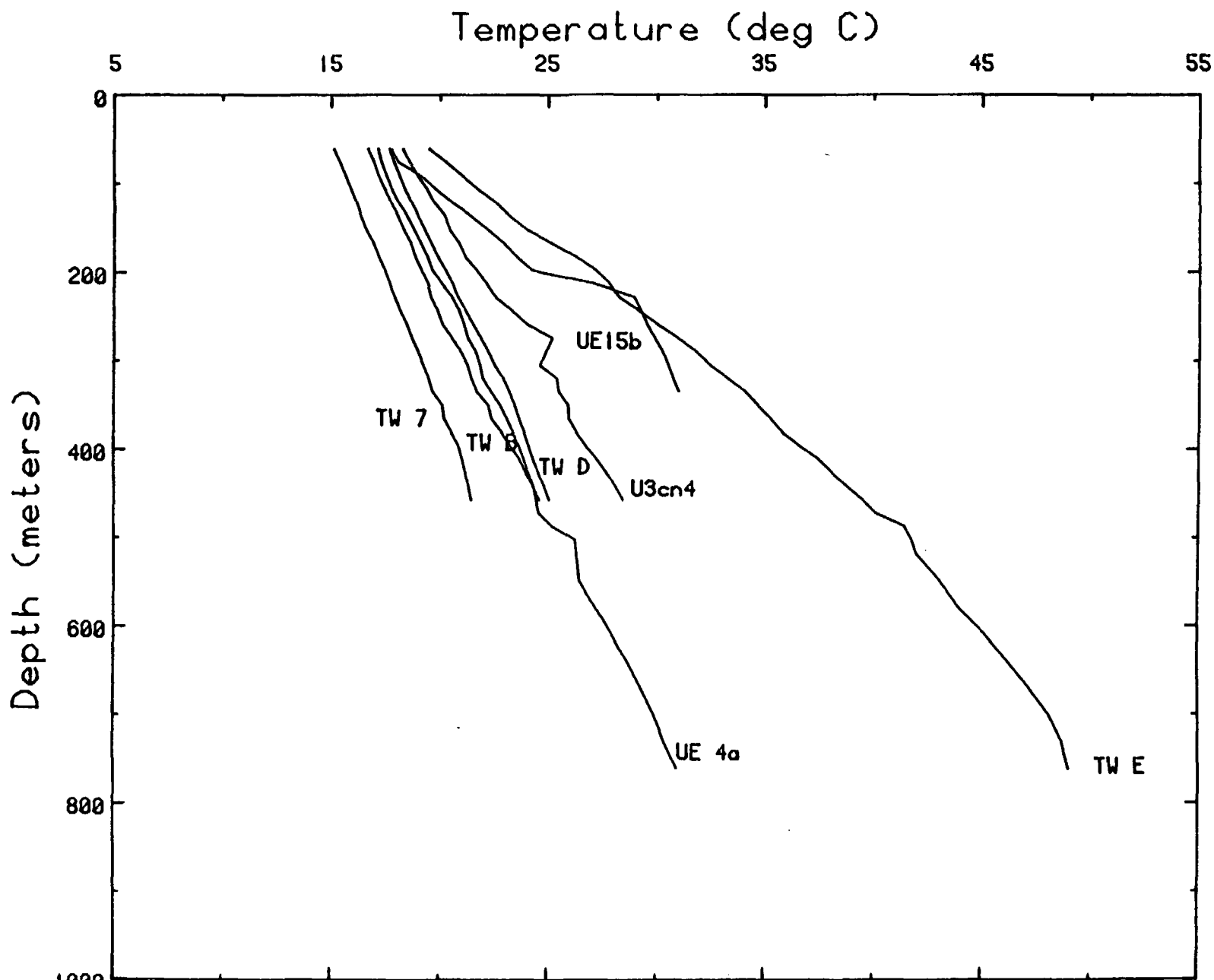

Figure 6. Composite Temperature Profile for Yucca Flat Area

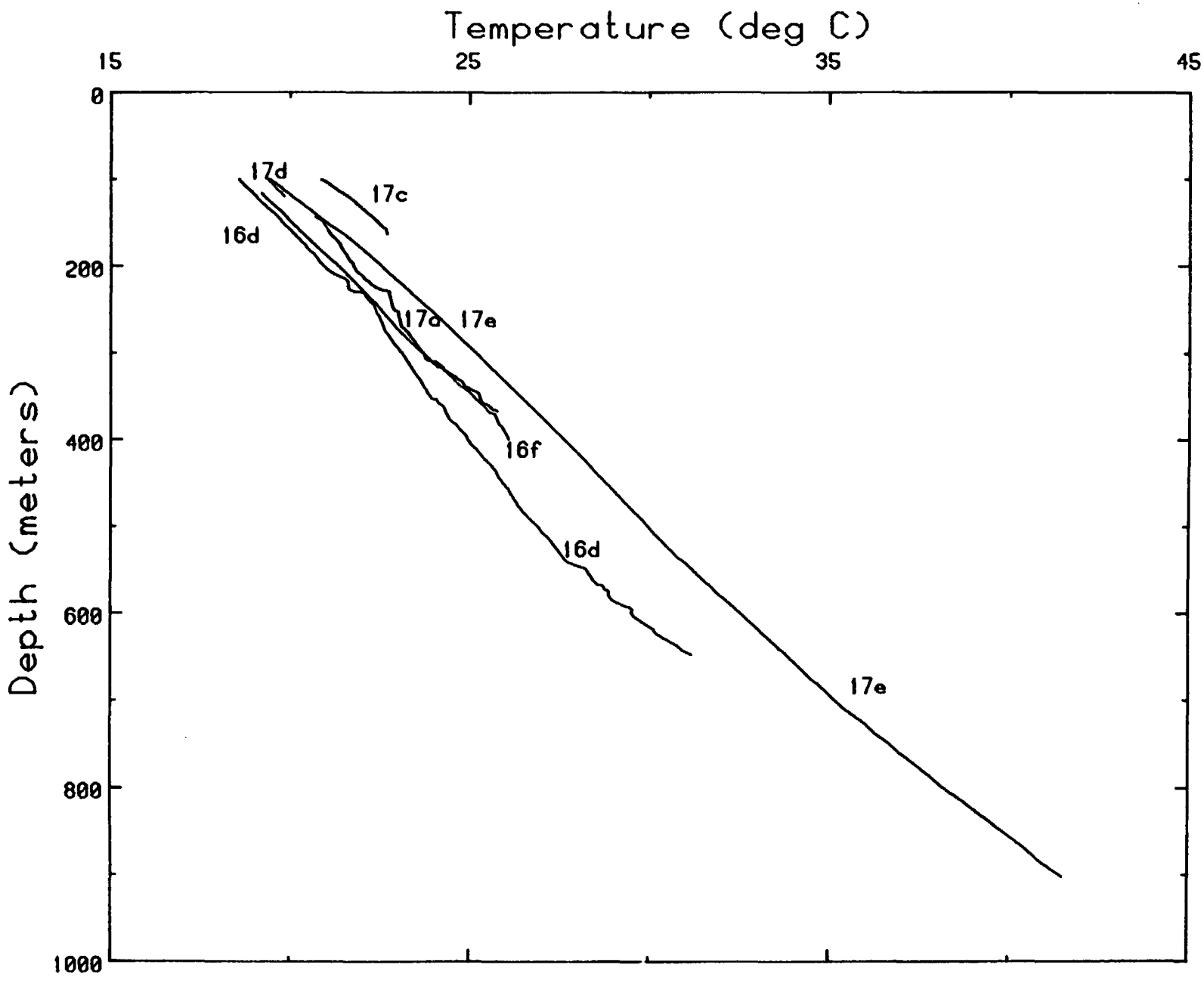

Figure 7. Composite Plot of Temperatures below 100 m, Syncline Ridge Area

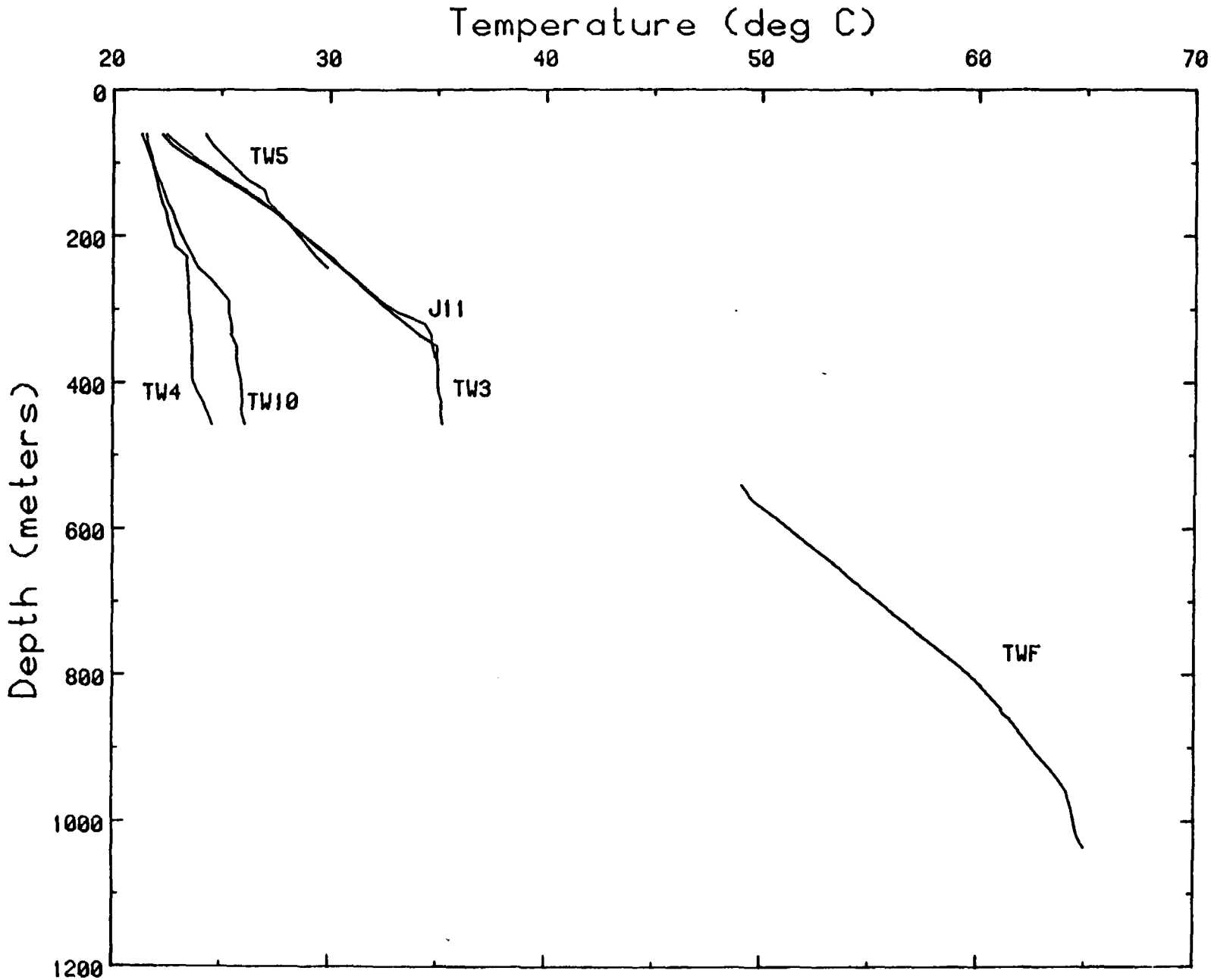

Figure 8. Composite Temperature Profile for the Southern NTS.

THERMAL REGIME OF YUCCA MOUNTAIN

Locations of wells drilled specifically to study the repository site being investigated at Yucca Mountain are shown in figure 9. The most recent temperature profiles from these wells (and some nearby wells, fig. 2) are presented in figures 10 and 11. The hydraulic potentiometric surface beneath Yucca Mountain is deeper than 500 meters. The curves show variations in thermal gradients to about 1,000 m. Thus, hydrologic disturbances to the temperature field may occur both above and below the water table. Some of the extreme variations in thermal gradient above the water table might be explained in terms of two-phase water flow, with the ratio of liquid to vapor varying as a function of depth (see Lachenbruch, 1981). At present, this seems to be the most reasonable physical explanation for the types of variations, both lateral and vertical, in temperature gradients observed in the "conductor holes" (UE25a4, 5, 6, and 7, fig. 9), a closely grouped series of holes drilled entirely within the unsaturated zone. Some, but by no means all, of the variations in gradient for this series (fig. 11) may be explained by long-lived transients resulting from the loss of large quantities of mud during drilling. The holes are, however, effectively in thermal equilibrium, and the gradient variations cannot be ascribed plausibly to variations in thermal conductivity (particularly where there are temperature reversals).

For the deepest wells (G1 and H1, fig. 10), systematic variations in temperature gradient occur without corresponding variations in thermal conductivity. Our preliminary interpretation suggested a systematic downward percolation of ground water through both unsaturated and saturated zones with seepage velocities of a few mm/y. With sufficient thermal conductivity data now available, we are able to test that interpretation quantitatively.

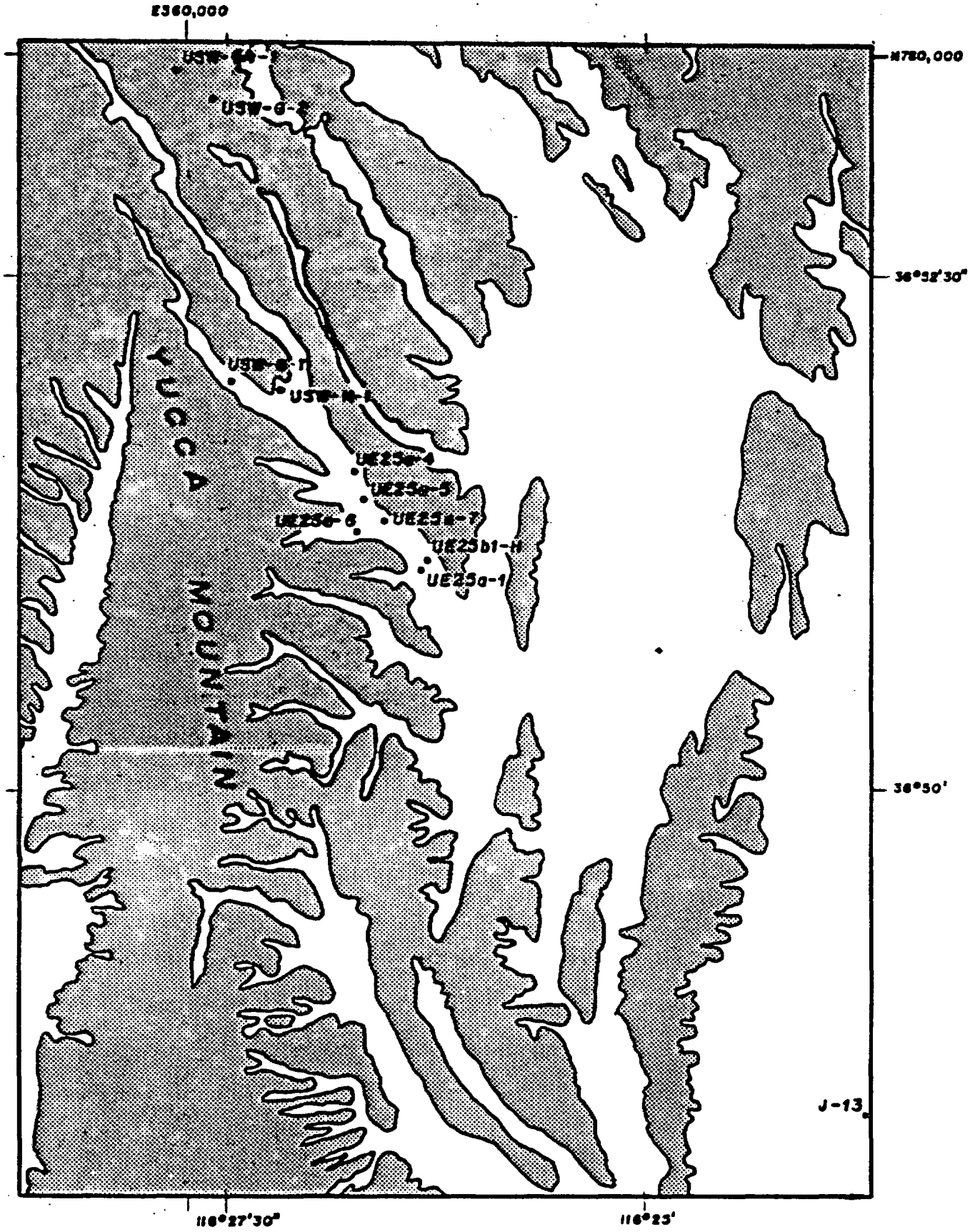

Figure 9. Locations of drill holes near Yucca Mountain.

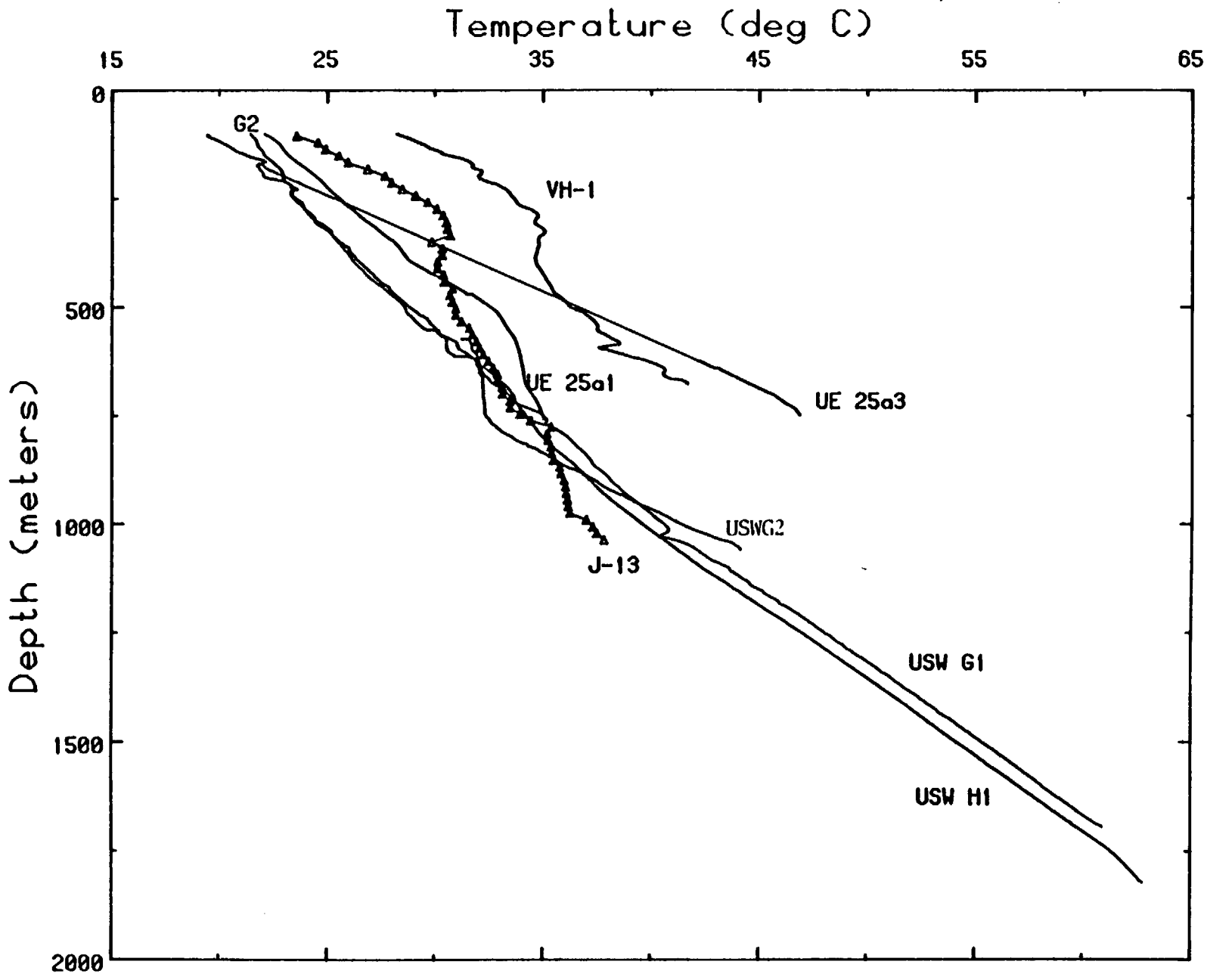

Figure 10. Temperatures in Wells deeper than 600 m, Yucca Mountain

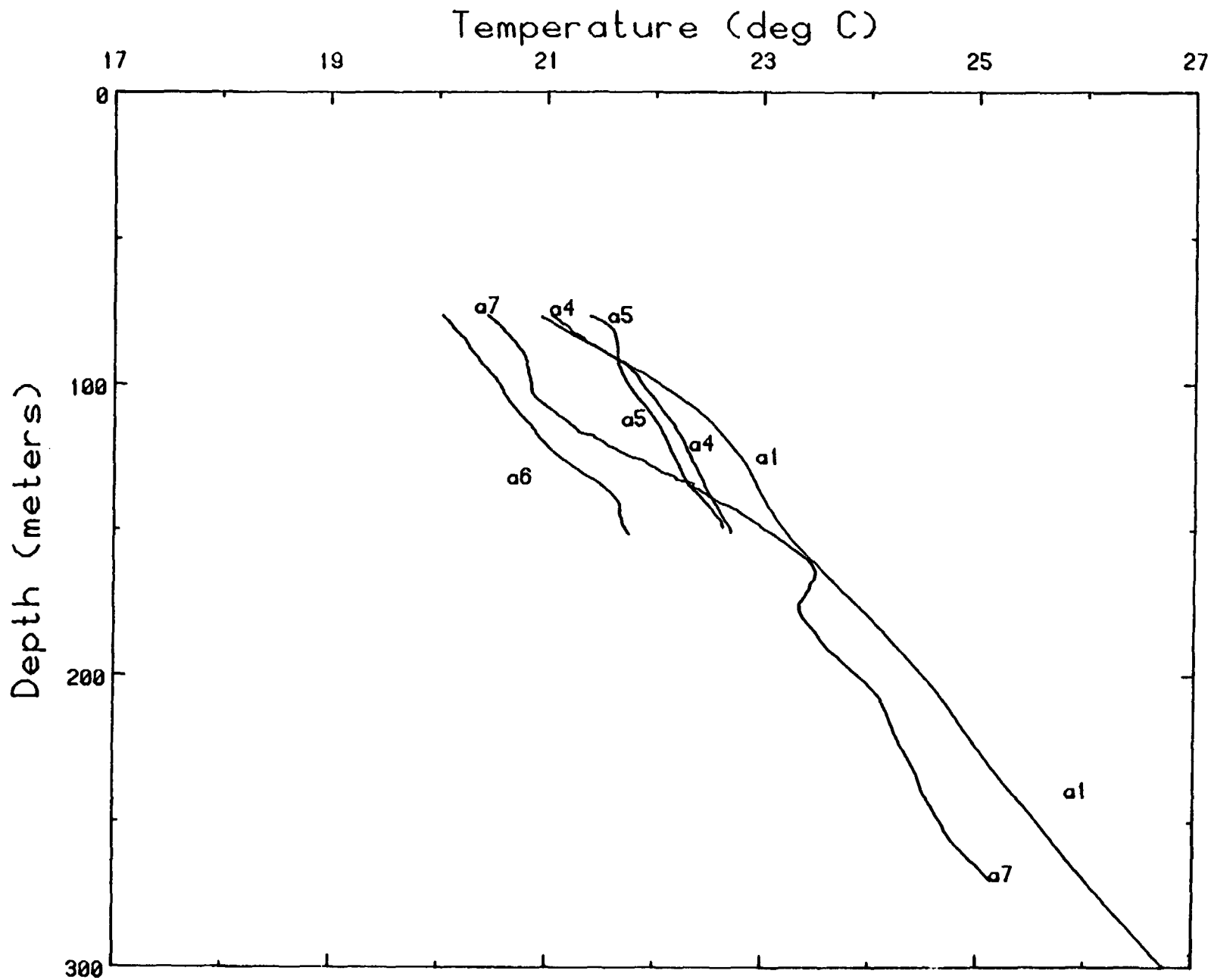

Figure 11. Temperatures from UE25a1 & the "conductor holes", Yucca Mtn.

Temperature gradients within individual formations were combined with thermal conductivity determinations by Lappin and others (1982) (above ~900 m) and our own measurements (below ~900 m) to obtain component conductive heat flows for each formation (table 2). The six interval heat flows increase systematically with depth, lending support to our preliminary interpretation. If we assume that one-dimensional steady-state vertical water flow is responsible for the observed increase in heat flow with depth and that the material is saturated, we may perform a simple calculation to estimate the seepage velocity and penetration depth of the vertical water flow.

For the idealized conditions assumed, conservation of mass and energy requires that the temperature θ be related to the vertical volumetric flow rate of interstitial water V by the differential equation (see e.g., Lachenbruch and Sass, 1977)

$$\frac{d}{dz}\, k\frac{d\theta}{dz} = -\rho' c' V \frac{d\theta}{dz} \qquad (1)$$

where z is depth and V is taken positive for upward flow. Density and specific heat at constant pressure for the water are represented by ρ' and c', respectively; k is thermal conductivity of the saturated aggregate. Their values are approximately

$$\rho' c' = 1 \text{ cal/cm}^3\ ^\circ\text{C} = 4.2 \times 10^6 \text{ J/m}^3\text{K} \qquad (2a)$$

$$k = 4.3 \text{ mcal/cm sec } ^\circ\text{C} = 1.8 \text{ W/m K} \qquad (2b)$$

The vertical conductive heat flow q (positive upward) is defined by

$$q = k\frac{d\theta}{dz} \qquad (3)$$

Combining (1) and (3) yields a relation between vertical heat flow and volumetric flow velocity V (e.g., cm^3 of water per cm^2 of cross sectional area

TABLE 2. Heat-flow determinations, USWG1

Depth interval m	Formation	Γ* °C km⁻¹	SE	N†	<K>†† Wm⁻¹ K⁻¹	SD	SE	Heat flow mWm⁻²	Heat flow HFU
91- 427	Paintbrush tuffs	16.32	0.08	0**	1.58	.30	.10	26±2	0.62
427- 549	Calico Hills tuffs	21.51	0.27	16**	1.31	0.11	0.03	28±1	0.67
610-1006	Crater Flat tuffs	23.01	0.08	27	1.65	0.28	0.05	38±1	0.91
1067-1204	Flow Breccia	31.16	0.19	4	1.65	0.26	0.13	51±4	1.23
1219-1524	Lithic-rich tuffs	29.04	0.03	10	1.81	0.13	0.04	53±1	1.26
1524-1697	Older tuffs	28.09	0.09	11	1.93	0.13	0.04	54±1	1.30

*Γ = least-squares temperature gradient ± Standard Error (SE).

†N = number of samples measured.

**These are estimates from Tables 9 and 10 of Lappin and others (1982).

††Harmonic mean thermal conductivity ± Standard deviation (SD) and Standard Error (SE) over the least-squares interval.

of aggregate per unit time)

$$\frac{dq}{dz} = -Aq \tag{4}$$

where

$$A = \frac{\rho' c' V}{k} \tag{5}$$

According to (4), the conducted heat flow at the surface q_o, is related to the conducted heat flow q(z) at depth z by

$$q(z) = q_o \, e^{-\bar{A}z} \tag{6}$$

where

$$\bar{A} = \frac{1}{z} \int_0^z A dz \tag{7}$$

Thus $\bar{A}$ is a representative value of A in the depth range [0,z].

To obtain an order of magnitude estimate of $\bar{A}$ (and hence V, equation 5), we neglect its variation with depth and fit a curve of form (6) to heat flows q(z) determined over a number of depth intervals in the hole. The interval heat flows were plotted as a function of the depth of the mid-point of the interval (fig. 12) and a least-squares regression curve (also shown in the figure) was calculated. The parameters of equation 6 obtained from the regression analysis are:

$$q_o = 0.53 \text{ HFU} = 22.4 \text{ mW/m} \tag{8}$$

$$\bar{A} = -6.12 \times 10^{-4} \text{ m}^{-1} \tag{9}$$

The correlation coefficient is 0.95, and the maximum departures from the least-squares line are about ±5 mW/m^2 which we consider reasonable in view of the idealized nature of the model and likely sources of measurement error.

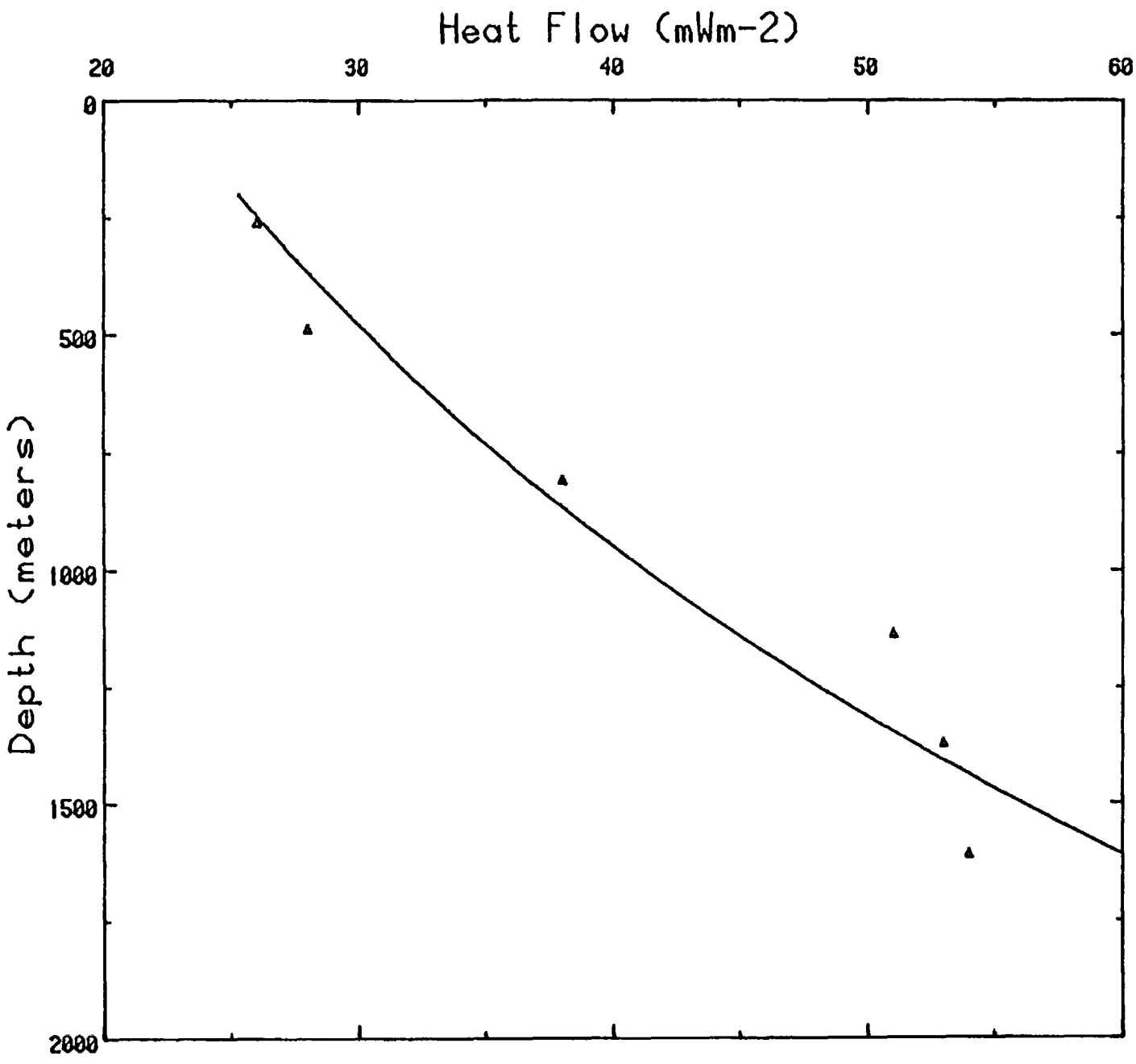

Figure 12. Interval heat flows (from Table 2) as a function of the depth of the midpoint of the interval. The least-squares regression line is $q = 22.4 \exp 6.12 \times 10^{-4} z$.

Combining equations 2, 5, and 9 yields an estimate of the vertical seepage velocity

$$V = \frac{-k}{\rho' c'} \bar{A} \qquad (10a)$$

$$= 2.6 \times 10^{-10} \text{ m/s} = 8 \text{ mm/y} \qquad (10b)$$

The average particle velocity of the pore water is obtained from V by dividing by the porosity; i.e., it would be 40 mm/yr (40 m/1000 yrs) for a porosity of 20% (10b).

If we assume that this simple flow pattern persists to some depth z^*, beneath which the heat flow is equal to the regional value $q(z^*)$, we can estimate the depth of vertical flow from equations 6, 8, and 9

$$z^* = \frac{-1}{\bar{A}} \ell n \frac{q(z^*)}{q_o} \qquad (11a)$$

$$\cong 2 \text{ km} \qquad \text{if } q(z^*) \cong 80 \text{ mW/m} \sim 2 \text{ HFU} \qquad (11b)$$

$$\cong 2.5 \text{ km} \qquad \text{if } q(z^*) \cong 100 \text{ mW/m} \sim 2.5 \text{ HFU} \qquad (11c)$$

Although this model represents a gross idealization, it leads to numerical values for vertical seepage velocity (10b) and circulation depth (11b and c) that are reasonable in order of magnitude and consistent with other information.

SUMMARY

From thermal measurements in about 60 wells, it appears that over much of the Nevada Test Site, including the Yucca Mountain site, the steady-state, conductive thermal regime has been altered significantly to depths as great as 2 to 3 km by water movement having a vertical component of seepage velocity of several meters per millenium. Regionally, the predominant vertical flow in this depth range is downward, but local upwellings exist. The measurements suggest 2- or 3-dimensional flow which in turn suggests that lateral movement of ground water must also be involved; however, the thermal measurements provide no measure of lateral velocities. In summarizing these results, we emphasize that of all the holes we have studied at NTS, only Ue17e was completed in the manner required for a confident analysis of the thermal effects of natural ground-water flow. In the other holes, the annulus was not blocked with grout, and uncertainties persist regarding possible complications of local vertical flow within the annulus behind the well casing.

In the Yucca Mountain area itself, measurements in wells deeper than 1 km suggest a downward water movement with seepage velocity on the order of 1-10 mm/y.

References

Lachenbruch, A. H., 1981, Temperature effects of varying phase composition during the steady vertical flow of moisture in unsaturated stratified sediments: U.S. Geological Survey Open-File Report 81-1220, 11 p.

Lachenbruch, A. H., and Sass, J. H., 1977, Heat flow in the United States and the thermal regime of the crust, in Heacock, J. H., ed., The Earth's Crust: American Geophysical Union Geophysical Monograph 20, American Geophysical Union, Washington, D. C., p. 626-675.

Lappin, A. R., Van Buskirk, R. G., Enniss, D. O., Butters, S. W., Prater, F. M., Muller, C. S., and Bergosh, J. L., 1982, Thermal conductivity, bulk properties, and thermal stratigraphy of silicic tuffs from the upper portion of hole USW-G1, Yucca Mountain, Nye County, Nevada: Sandia National Laboratories Report SAND 81-1873.

Sass, J. H., Blackwell, D. D. Chapman, D. S., Costain, J. K., Decker, E. R., Lawver, L. A., and Swanberg, C. A., 1981, Heat flow from the crust of the United States, in Touloukian, Y. S., Judd, W. R., and Roy, R. F., eds., Physical Properties of Rocks and Minerals: McGraw-Hill Book Company, p. 503-548.

Sass, J. H., Lachenbruch, A. H., and Mase, C. W., 1980, Analysis of thermal data from drill holes UE25a-3 and UE25a-1, Calico Hills and Yucca Mountain, Nevada Test Site: U.S. Geological Survey Open-File Report 80-826, 25 p.

Sass, J. H., Lachenbruch, A. H., Munroe, R. J., Greene, G. W., and Moses, T. H., Jr., 1971, Heat flow in the western United States: Journal of Geophysical Research, v. 76, p. 6376-6413.

Swanberg, C. A., and Morgan, P., 1978, The linear relation between temperature based on the silica content of groundwater and regional heat flow: A new heat flow map of the United States: Pure and Applied Geophysics, v. 117, p. 227-241.

Winograd, I. J., and Thordarson, W., 1975, Hydrogeologic and hydrochemical framework, South-Central Great Basin, Nevada-California, with special reference to the Nevada Test Site: U.S. Geological Survey Professional Paper 712-C, 126 p.

APPENDIX A-1.

Thermal conductivity, density, and apparent porosity of tuffs from USWG1 (measured at ~25°C)

TABLE A-1. Thermal conductivity, density, and apparent porofity of tuffs from USWG1 (measured at ~25°C)

Depth, m	Formation	Lithology	K $Wm^{-1} K^{-1}$	$\rho^{\dagger}$ $gm\ cm^{-3}$	$\phi^{\dagger\dagger}$ %
868.1	TcfT	Moderately welded tuff	1.80	2.20	22.2
892.8	TcfT	Moderately welded tuff	1.94	2.34	15.3
892.9	TcfT	Moderately welded tuff	1.87	2.36	15.7
899.8	TcfT	Moderately welded tuff	1.87	2.37	13.7
930.2	TcfT	Moderately welded tuff	1.42	2.11	22.4
940.4	TcfT	Moderately welded tuff	1.54	2.13	20.4
967.3	TcfT	Zeolitized partially welded tuff	1.62	2.29	16.6
983.6	TcfT	Zeolitized non-welded tuff	1.67	NM	NM
1013.8	TcfT	Vitrophyre	1.67	2.29	18.2
1044.5	TcfT	Vitrophyre	2.00	NM	NM
1065.6	TcfT	Vitrophyre	1.80	2.34	15.6
1091.6	Tfb	Flow Breccia	1.86	2.44	12.1
1123.4	Tfb	Flow Breccia	1.43	2.34	14.5
1157.9	Tfb	Flow Breccia	1.95	2.55	3.2
1187.9	Tfb	Flow Breccia	1.49	2.34	12.5
1219.4	Trt	Zeolitized partially welded tuff	1.65	2.19	15.7
1253.6	Trt	Zeolitized partially welded tuff	1.80	2.25	13.6
1280.1	Trt	Zeolitized partially welded tuff	1.88	2.16	16.5
1319.9	Trt	Zeolitized partially welded tuff	1.72	2.24	16.7
1349.2	TrT	Zeolitized partially welded tuff	1.77	2.23	15.4
1389.4	TrT	Zeolitized partially welded tuff	1.86	2.32	14.5
1419.3	TrT	Zeolitized partially welded tuff	1.75	2.27	16.8
1450.7	TrT	Zeolitized partially welded tuff	1.96	2.37	11.0
1477.5	TrT	Zeolitized non-welded tuff	2.10	NM	NM

TABLE A-1. Thermal conductivity, density, and apparent porosity of tuffs from USWG1 (measured at ~25°C)--continued

Depth, m	Formation	Lithology	K $Wm^{-1} K^{-1}$	$\rho^{\dagger}$ $gm\ cm^{-3}$	$\phi^{\dagger\dagger}$ %
1511.6	TrT	Zeolitized non-welded tuff	1.68	NM	NM
1540.0	TtA	Silicic tuff densely welded	1.98	2.30	12.4
1573.0	TtA	Silicic tuff densely welded	1.98	2.28	14.0
1600.0	TtA	Zeolitized tuff densely welded	2.15	2.30	14.8
1632.6	TtB	Zeolitized tuff bedded	2.12	2.35	11.3
1675.7	TtC	Zeolitized non-welded tuff	1.70	NM	NM
1716.9	TtC	Zeolitized tuff densely welded	1.94	2.39	11.2
1747.7	TtC	Devitrified moderately welded tuff	1.91	2.46	9.2
1754.5	TtC	Devitrified moderately welded tuff	1.85	2.43	11.0
1783.3	TtC	Devitrified moderately welded tuff	1.97	2.47	8.6
1813.8	TtC	Silicified moderately welded tuff	1.89	2.49	5.8
1814.0	TtC	Silicified moderately welded tuff	1.86	2.31	13.6

*TcfT, tram unit, Crater Flat tuff
Tfb, Flow Breccia
TrT, Lithic-rich tuff
Tt, older ash-flow and bedded tuff, units A, B, and C

†Saturated density NM, not measured (because of disintegration of specimen).

††Apparent porosity = $\frac{\text{saturated weight - dry weight}}{\text{saturated weight}}$ NM, not measured.